Available online at www.sciencedirect.com
SCIENCE DIRECT®
Journal of Nuclear Materials 321 (2003) 8–18
journal of nuclear materials
www.elsevier.com/locate/jnucmat

Contribution to a thermodynamic database and phase equilibria calculations for low activation Ta-containing steels

A. Danon, C. Servant *

Laboratoire de Physico-Chimie de l'Etat Solide, Faculté de Sciences d' Orsay, Université de Paris-Sud, Bât 410, 91405 Orsay cedex, France

Received 9 December 2002; accepted 12 March 2003

Abstract

In the framework of the Calphad-Thermocalc approach, a first attempt is presented to update the TCFe2000 steel database by introducing existing and recently optimized thermodynamic parameters of Ta-containing binary and ternary systems. The ultimate aim of the work is to develop a self-consistent thermodynamic description of low-activation steels. In a first stage, we performed a complete modeling and optimization of the Fe–Ta binary system in order to provide a description of its intermediate phases coherent with that existing for other systems in the TCFe2000 database. In doing such a modeling, we have also taken into account experimental data of higher order systems such as Fe–Ta–C and Fe–Ta–N. After considering the reported interactions of Ta with other alloying elements of low-activation steels, we have carried out phase diagram calculations in the austenite region of the Eurofer 97 (9CrWVTa) alloy. A reasonable agreement was found with the available experimental information.

1. Introduction

Martensitic 7–12 Cr steels have been extensively studied as structural materials for different applications in thermal power plants, pipe lines, etc., due to their high strength and ductility at normal service temperatures. In the past decade, CrWVTa martensitic steels were developed for specific applications to internal components of fusion reactors, owing to an attractive combination of properties such as good stability and lower induced activity under neutron irradiation [1,2]. The concept of reduced activation implied the addition of alloying elements that, when irradiated, form radioactive products whose activity decays to low levels in tens of years instead of thousands of years. To meet this criterion, Mo, Nb, Ni, Cu and N must be eliminated or reduced in these steels.

Reduced activation steels are variations of conventional ferritic/martensitic steels, with molybdenum replaced by tungsten and niobium replaced by tantalum. The role of Ta in the evolution of the microstructure and its effect on mechanical properties after different schedules of thermomechanical processing has been the object of studies, either for tempering or aging [2–4] as well as for austenitization treatments [2,5,6].

The first low-activation martensitic steel manufactured at an industrial scale in Europe is Eurofer 97 (9CrWVTa). Some aspects of the behavior of this alloy, including the metallurgical characterization of the as-received condition [7], continuous cooling transformations [8] and mechanical tests [9] have been previously reported. 'Dynamic' pinning effects due to the presence of Ta-rich particles (carbides, nitrides or carbonitrides) are probably responsible for the highly heterogeneous austenite grain size found in specific austenitizing conditions [10].

* Corresponding author. Tel.: +33-1 6915 7021; fax: +33-1 6915 7833.
E-mail address: colette.servant@lpces.u-psud.fr (C. Servant).

0022-3115/$ - see front matter © 2003 Elsevier B.V. All rights reserved.
doi:10.1016/S0022-3115(03)00196-X

To our knowledge, the only work in the previous literature concerning thermodynamic calculations using the Thermocalc software in Ta-containing low-activation steels is that in Ref. [3], which dealt with the tempered state of 5 to 9Cr2WTa steels. The authors did not specify the characteristics of the thermodynamic database they used.

The aims of the present work are:

(i) to contribute to the improvement of the TCFe2000 SGTE thermodynamic database for steels by adding in a consistent way existing and recently optimized thermodynamic data that concern Ta-containing systems,
(ii) to use the updated database to calculate phase equilibria of Eurofer97 or similar steels at austenite annealing temperatures, as a contribution to clarify the role of Ta-rich particles in the development of the austenite microstructure under dynamic conditions.

2. Material and thermodynamic calculations

The chemical composition of the Eurofer 97 alloy (in wt%) is: C (0.12), Cr (8.96), W (1.04), Ta (0.15), V (0.18), Mn (0. 48), Si (0.03), Ni (0.06), N (0.022), Nb (<0.002). For the quoted austenitization studies, the as-received metallurgical state was normalized at 980 °C for 31 min and tempered at 760 °C for 90 min. The corresponding microstructure had been previously characterized as being 100% martensite, with $M_{23}C_6$ carbides containing ≈56% Cr, up to 15% W, ≈1–2% V and no Ta, and Ta-rich particles (Ta 90%) containing up to 6% Cr, ≈1–2% V and no W [10].

Phase equilibria were investigated under the CALPHAD approach [11] using the Thermocalc software [12] coupled with the SGTE TCFe2000 thermodynamic database for steels. The optimization process was carried out using the Parrot module. A first attempt was done to construct an updated subset of this database by introducing the optimized thermodynamic parameters reported in the literature for the following Ta-containing systems: C–Ta [13], N–Ta and C–N–Ta [14], Cr–Ta [15], Cr–Ni–Ta [16], Cr–Ta–W [17] and Si–Ta [18].

We have not included the thermodynamic parameters given in Ref. [19] for the Ta–V system, where the Laves phase was considered as a stoichiometric compound; as shown below, the Laves phases considered in the present work have a composition range. In view of that, further work on that system is currently in progress.

Despite the fact that the Fe–Ta binary system has been already modeled [20,21], we have completely recalculated it in order to get a description of the μ phase consistent with that existing in the TCFe2000 database.

2.1. Thermodynamic phase modeling

We have used the same thermodynamic model to describe the same phase in the different involved systems. The thermodynamic descriptions of elements were taken from the SGTE database [22].

2.1.1. Solution phases

The solution phases (liquid, bcc A2 and fcc A1) were modeled as a substitutional solution according to the polynomial Redlich–Kister model [23].

2.1.2. Intermediate phases in the Fe–Ta binary system

The ε *Laves phase* (prototype $MgZn_2$, Pearson symbol hp12, Strukturbericht C14) contains three sublattices from the crystallographic point of view. To simplify the thermodynamic description of this phase, only two sublattices were considered by combining all sites with coordination number 12 (Wyckoff symbols: 2(a) and 6(h)) into one sublattice and the site with coordination number 16 (4f) into a second sublattice, obtaining in this way a stoichiometry 2-1. The accepted criterion to define the reference state for the thermodynamic functions is to assign the fcc reference state to species occupying a site with coordination 12 and the bcc reference state to species occupying a site with coordination > 12. This is true for the systems Fe–Nb and Fe–W in the current status of the TCFe2000 database. However, to keep the coherence with the existing description of the Laves phase in the Cr–Ta [15] and Cr–Ni–Ta [16] systems, we have defined the reference state for the thermodynamic functions as bcc Fe and bcc Ta, irrespective of the coordination number. In addition, the Wagner–Schottky addition rule for sublattices [24] was used to describe the Laves phase of the Fe–Ta binary system, as was done in those two systems:

$$ {}^{0}G^{\mathrm{LavesC14}}_{\mathrm{Ta:Fe}} = -{}^{0}G^{\mathrm{LavesC14}}_{\mathrm{Fe:Ta}} + {}^{0}G^{\mathrm{LavesC14}}_{\mathrm{Fe:Fe}} + {}^{0}G^{\mathrm{LavesC14}}_{\mathrm{Ta:Ta}}. \quad (1) $$

On the other hand, the Wagner–Schottky model is not followed in the current description of the the Fe–Nb and Fe–W systems.

The molar Gibbs energies of formation of the hypothetical phase formed with pure elements were fixed at the value 5000 J/mol of atoms in order to be consistent with other systems like Cr–Ti [25] or Cr–Nb [26].

Since the experimental homogeneity range of the Laves phase extends on both sides of the stoichiometric composition, the adopted unit formula for its description was $(Fe,Ta)_2$ (Fe,Ta). A congruent melting point was assumed for the Laves phase.

The μ *phase* (prototype Fe_7W_6, Pearson symbol hR13) contains five independent sublattices with 1, 2, 2, 2 and 6 sites per unit cell having coordination numbers 12, 15, 16, 14 and 12 and Wyckoff symbols 1(a), 2(c), 2(c), 2(c), 6(h), respectively. For the sake of simplicity

and coherence with existing data in the TCFe2000 database, we reduced the number of sublattices to three, grouping both sites of coordination number 12 into one sublattice and two sites 2(c) into another. The last sublattice was reserved to the remaining site 2(c). We assumed a congruent melting point as well. In order to account for the homogeneity range of this phase we have chosen the thermodynamic modeling $(Fe,Ta)_7Ta_2$ (Fe, $Ta)_4$. In this case also, we applied the Wagner–Schottky principle, writing

$$^0G^{\mu}_{Fe:Ta:Fe} = -^0G^{\mu}_{Ta:Ta:Ta} + {}^0G^{\mu}_{Fe:Ta:Ta} + {}^0G^{\mu}_{Ta:Ta:Fe}. \quad (2)$$

We kept the same value of 5000 J/mol of atoms for the Gibbs energy of formation of the hypothetical phase formed with pure elements. The reference state of Fe in the thermodynamic functions was fcc for the site with coordination number 12; we have chosen the bcc reference state of Ta, irrespective of the occupied site.

2.1.3. Carbides, nitrides, carbonitrides

The fcc M(C,N) carbonitride phase and derived phases as carbides and nitrides were described using a two-sublattice model with unit formula $(M_1,\ldots,M_n)$ (C,N,Va) where $M_1,\ldots,M_n$ stand for the metal atoms mixed in the substitutional sublattice and C, N and Va are located in the interstitial sublattice. The same unit formula and model parameters were used for the fcc solid solution phase; actually, the fcc + M(C,N) two-phase region is regarded as a miscibility gap in the fcc phase.

Other work has reported a different method to treat the problem of unmixing in the fcc structure. Thus, Akamatsu et al. [27] considered a different fcc phase (without Fe) to describe the carbonitride in a FeNb-TiCN, interstitial-free steel system, allowing in turn a miscibility gap to exist for this phase. They mentioned the possibility of stability problems in calculations to justify this procedure.

As explained below, unmixing phenomena giving rise to more than two fcc phases – i.e., the decomposition of a complex carbonitride in two simple carbonitrides – are only marginally treated in this first approach.

We have not considered the possibility of substituting Ta for other alloying elements in the $M_{23}C_6$ carbide, which was modeled with three sublattices in the TCFe2000 database. Our STEM measurements on thin foils of the as received alloy Eurofer 97 seem to sustain this assumption. On the other hand, carburization of ferrotantalum or prolonged annealing of powder compacts of Ta and cementite showed that Ta does not substitute for Fe in cementite, nor does it form a double carbide of any type of the form $(Fe,Ta)_xC_y$ [28,29].

We have introduced the following notation for the carbonitride-like phases when results are expressed in atomic fraction: Ta(V)C(N) will indicate a simple Ta carbide with traces of V and N; in the same way V(Ta)N(C) will mean a vanadium nitride with minor Ta and C. On the other hand (Ta,V)C(N) will account for a complex carbide in which Ta and V are present in similar proportions (that is, in the same order of magnitude) with low amounts of N, while (Ta,V)(C,N) indicates a carbonitride of Ta and V.

2.2. The Fe–Ta binary system

2.2.1. Why to reassess the Fe–Ta binary phase diagram?

Conflicting information existed in previous modeling with respect to the melting behavior and homogeneity range of the ε and μ phases of the Fe–Ta binary system. Ref. [20] accounts for a Laves phase ε with a congruent melting point and a homogeneity range of nearly 10 at.%; while the μ phase appears as a stoichiometric compound with a congruent melting point. On the other hand, in Ref. [21], the ε phase melts peritectically and the μ phase presents a stability range in composition. In addition, since our interest was finally focused on steel systems, it was important to achieve a model of this particular binary system consistent with available data of systems of higher order. For instance, the stability of the fcc (Fe,Ta) binary phase was found to play a crucial role on the carbide or nitride solubility in a (Fe,Ta,C or N) austenite when coupled with the thermodynamic descriptions of Refs. [13,14]. A similar difficulty was quoted by Lee [30] for the solubility products of NbC and NbN in an Fe–Nb austenite at low temperatures in studying the system Fe–Nb–Ti–C–N. This author dealt with the problem by reassessing the binary system Fe–Nb in order to make the fcc solid solution more stable at low temperatures, and changing slightly the stability of the NbC carbide in the Nb–C binary system as well.

For these reasons and as a first stage of a broader project, we decided to fully recalculate the Fe–Ta binary system assuming the description of the intermediate phases given in Section 2.1.2 and taking into account the solid solubility data for carbides and nitrides in austenite in the ternary systems Fe–Ta–C and Fe–Ta–N, respectively. For this to be accomplished, we searched in a first step for a set of thermodynamic parameters of the fcc (Fe,Ta) binary phase able to fit the experimental data in the ternary systems Fe–Ta–C and Fe–Ta–N by combining the thermodynamic description of the Fe–Ta binary system and that of the Ta–C [13], Ta–N [14] and Ta–C–N [14] systems. In a second step, we proceeded with the optimization of the rest of the Fe–Ta binary phases fixing the values of the parameters found for the fcc phase. In this way, the solid solubility ternary data turned out to be an additional constraint in the evaluation of the binary thermodynamic parameters. This fact restrained severely the possibilities for obtaining the most accurate description of the whole binary system.

2.2.2. Available experimental binary and ternary data

The experimental binary data taken into account to model the Fe–Ta binary system were: (i) The data for the enthalpy of mixing of the liquid of Iguchi et al. [31] at 1593 °C. Data of Sudavtsova et al. [32] at 1657 °C were discarded for the reasons exposed in Ref. [21]. (ii) The data for the activity and chemical potential of Ichise and Horikawa [33] at 1600 °C. (iii) The boundaries of two-phase fields given by Raman [34], Coelho et al. [35] and Ichise and Horikawa [33] at 1300, 1400 and 1600 °C, respectively. (iv) The data for the solubility of Ta in Fe of Fischer et al. [36], Abrahamson and Lopata [37] and Sinha and Hume-Rothery [38]; data on the solubility of Genders and Harrison [39] were not taken into account.

As for ternary systems, to our knowledge the only available experimental data on the solubility of tantalum carbides or nitrides in austenite are those of Narita [40] and Mori et al. [41] for ternary FeTaC and FeTaN alloys. Additional data were published by Tamura et al. [6] for a series of CrWVTa steels. These experimental data were obtained by applying the following equations for the solubility product of TaC and TaN in austenite:

$$\log[\%\mathrm{Ta}][\%\mathrm{C}] = -7027/T + 3.16 \text{ [6]}, \tag{3}$$

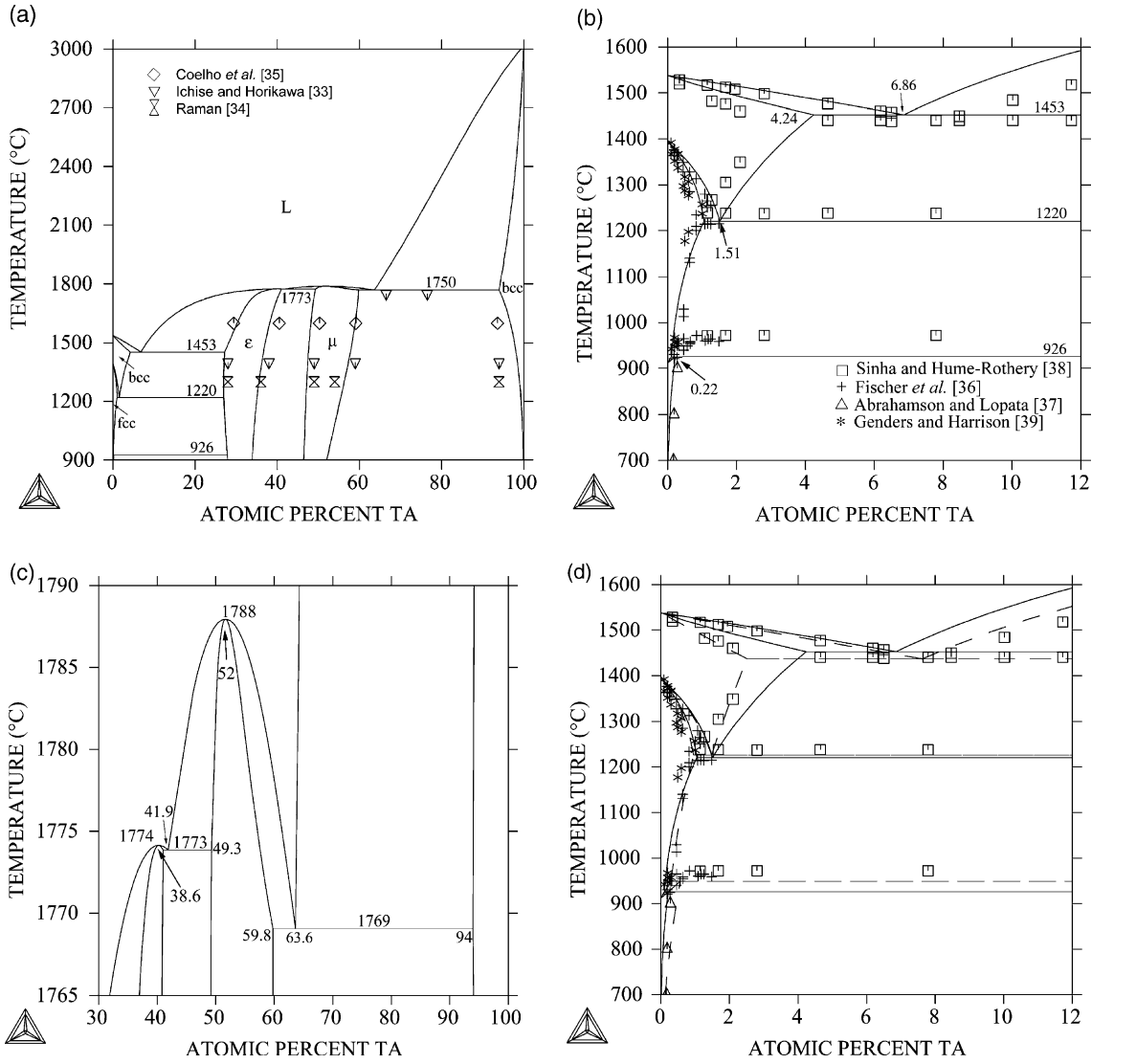

Fig. 1. Calculated Fe–Ta phase diagram and experimental data. (a) Fe–Ta binary phase diagram. (b) Iron rich corner. (c) Congruent points for the Laves and μ phases. (d) Comparison between diagrams obtained by taking into account only binary data (dashed line) and both binary and ternary data (full line).

Table 1
Calculated and measured values for invariant equilibria in the Fe–Ta system

Equil. phases	React.	T (°C)		Composition (at.% Ta)		Ref. (Exp.)	Ref. (calc.)	Calc. (this work)	
		Exp.	Calc.	Exp.	Calc.			Temp. (°C)	Comp. (at.% Ta)
$\mu \leftrightarrow$ Liq.	C	1870[a]		51.6		[42]			
			1884		53.82		[21]	1788	52
			1776		53.84		[20]		
Liq. + $\mu \leftrightarrow \varepsilon$	P		1816		L 42.88 μ 50.79 ε 43.62		[21]		
$\varepsilon \leftrightarrow$ Liq.	C	1775		32.6		[43]			
			1762		33		[20]	1774	38.6
Liq. $\leftrightarrow \mu$ + bcc	E	1750				[35]			
			1747		L 68.34 μ 59.3 bcc 93.62		[21]	1769	L 63.6 μ 59.8 bcc 94
			1592		L 68.34 μ 53.84 bcc 95.0		[20]		
$\varepsilon + \mu \leftrightarrow$ Liq.	E		1722		ε 36.6 μ 53.84 L 42		[20]	1773	ε 41 μ 49.3 L 41.9
		>1617				[33]			
		1530–1570				[44]			
Liq. $\leftrightarrow \varepsilon$ + bcc(δ)	E		1442		L 7.97 ε 27.29 δ 1.82		[21]	1453	L 6.86 ε 27.2 δ 4.24
		1441 ± 2				[33]			
		1440 ± 2		L 7.9 ε 33.3 δ 2.8		[38]			
			1430	L 7.9 ε 26.5 δ 2.4			[20]		
bcc(δ) $\leftrightarrow \varepsilon + \gamma$	EO	1239 ± 2		δ 1.1 ε 33.33 γ 0.5		[38]			
			1228		δ 1.31 ε 26.8 γ 0.83		[20]		
		1220		δ 1.45 ε 3.33 γ 0.96		[39]		1220	δ 1.5 ε 27 γ 1
			1216		δ 1.34 ε 28.99 γ 0.81		[21]		
		1215		δ 1.38 ε 33.33 γ 0.86		[36]			
bcc(α) $\leftrightarrow \gamma + \varepsilon$	PO		977		α 0.8 γ 0.43 ε 30.82		[21]		
		972 ± 3		α 0.6 γ 0.3 ε 33.33		[38]			

Table 1 (*continued*)

Equil. phases	React.	T (°C)		Composition (at.% Ta)		Ref. (Exp.)	Ref. (calc.)	Calc. (this work)	
		Exp.	Calc.	Exp.	Calc.			Temp. (°C)	Comp. (at.% Ta)
		965		α 0.71 γ 0.4 ε 33.33		[36]			
		974		α 0.32 γ 0.2 ε 33.33		[39]			
			947		α 0.46 γ 0.2 ε 27.6		[20]	926	α 0.22 γ 0.1 ε 27.86

C: congruent melting point, E: eutectic, P: peritectic, EO: eutectoid, PO: peritectoid.
[a] Evaluated temperature.

$$\log[\%\mathrm{Ta}][\%\mathrm{C}] = -7000/T + 2.90 \text{ [40]}, \quad (4)$$

$$\log[\%\mathrm{Ta}][\%\mathrm{N}] = -12\,800/T + 6.08 \text{ [40]}, \quad (5)$$

$$\log[\%\mathrm{Ta}][\%\mathrm{N}]^{0.85} = -7400/T + 2.09 \text{ [41]}, \quad (6)$$

where T is in K and % is in weight. Mori's equation (6) for TaN [41] includes a coefficient that accounts for substoichiometry. According to himself, his equation for TaC gives similar results to Narita's one, so that we have just considered Narita's results.

3. Results and discussion

3.1. Calculation of the Fe–Ta binary system

Fig. 1 shows the result of the new optimization; the values of the new thermodynamic parameters are presented in the Appendix A. To illustrate the difficulties quoted in Section 2.2.1 above, we compare in Fig. 1(d) the results of two different calculations of the Fe–Ta system, that is, the one performed by taking into account binary and ternary data (full line, i.e., the adopted diagram) and one performed by taking into account only binary data (dashed line). The diagram shown in dashed line fits more accurately the experimental data, but the binary parameters optimized in that case completely fail to reproduce the ternary data in the Fe–Ta–C and Fe–Ta–N systems when combined with the thermodynamic parameters of Refs. [13,14], as will be shown in the next section. The previously measured and calculated values for the invariant equilibria of the Fe–Ta binary system taken from the above mentioned references and Refs. [42–44] are given in Table 1, along with the corresponding values calculated in the present work.

Figs. 2 and 3 show the results of calculations of the enthalpy of mixing of the liquid phase and the activity of Fe and Ta in the different phase fields using the new thermodynamic parameters; Fig. 4 displays the chemical potential of Fe and Ta. For enthalpy calculations we considered liquid Fe and Ta as reference states at 1593 °C; for activity and potential calculations we used liquid Fe and bcc Ta as reference states at 1600 °C.

The calculated diagram of Fig. 1 shows a reasonable agreement with experimental data in the iron-rich region and for the boundaries of intermediate phase fields; however, the peritectoid temperature of 926 °C is somewhat lower and the stability of the bcc phase at high temperatures somewhat higher than the corresponding experimental values (see Table 1). The calculated enthalpy of mixing of the liquid phase fits the experimental data of Ref. [31], unfortunately determined

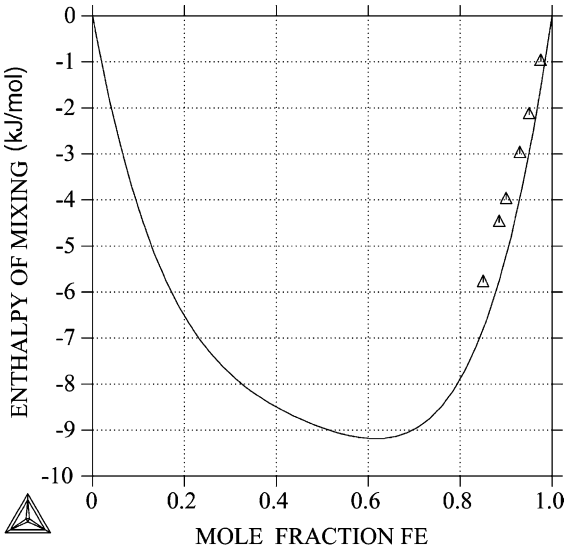

Fig. 2. Enthalphy of mixing of the liquid at 1593 °C.

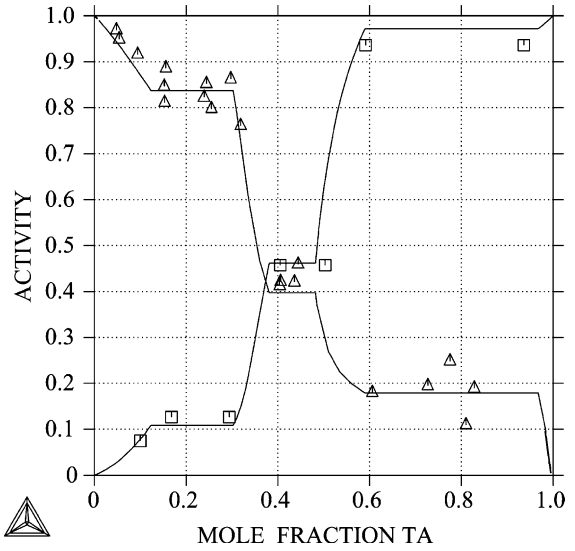

Fig. 3. Activity of Fe and Ta in the different phase fields at 1600 °C.

only in the Fe-rich region. The calculated chemical potential and activity of Fe and Ta are also in satisfactory agreement with the experimental ones.

On the other hand, the type and location of some invariant points should be experimentally confirmed. In particular, the melting behavior of the ε and μ phases, as pointed out in Ref. [35], has to be clarified; the eutectic reaction between these phases calculated in the present work could be easily transformed into a peritectic one.

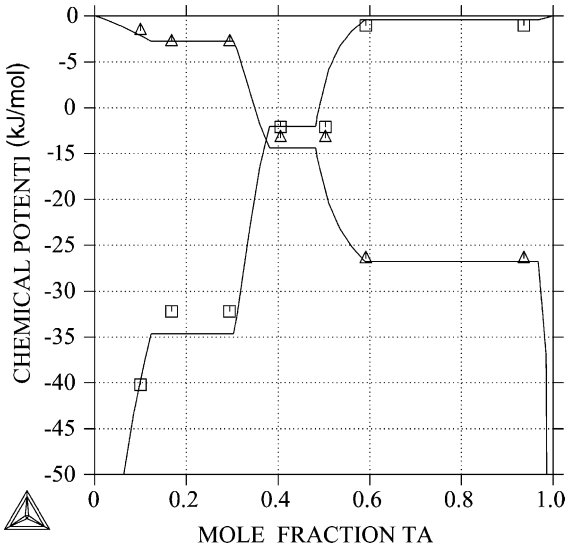

Fig. 4. Chemical potential of Fe and Ta in the different phase fields at 1600 °C.

3.2. Phase equilibria in austenite

3.2.1. Calculated equilibrium solubility of Ta-rich carbides in austenite

Fig. 5 compares the solubility curves for TaC in a (Fe,Ta) austenite calculated by Thermocalc to those extracted from Naritas's equation at $T = 1050$ and 1200 °C. We have also plotted in Fig 5(b) the curve resulting from the optimization shown in dashed line in Fig. 1(d), that is, taking into account only binary experimental

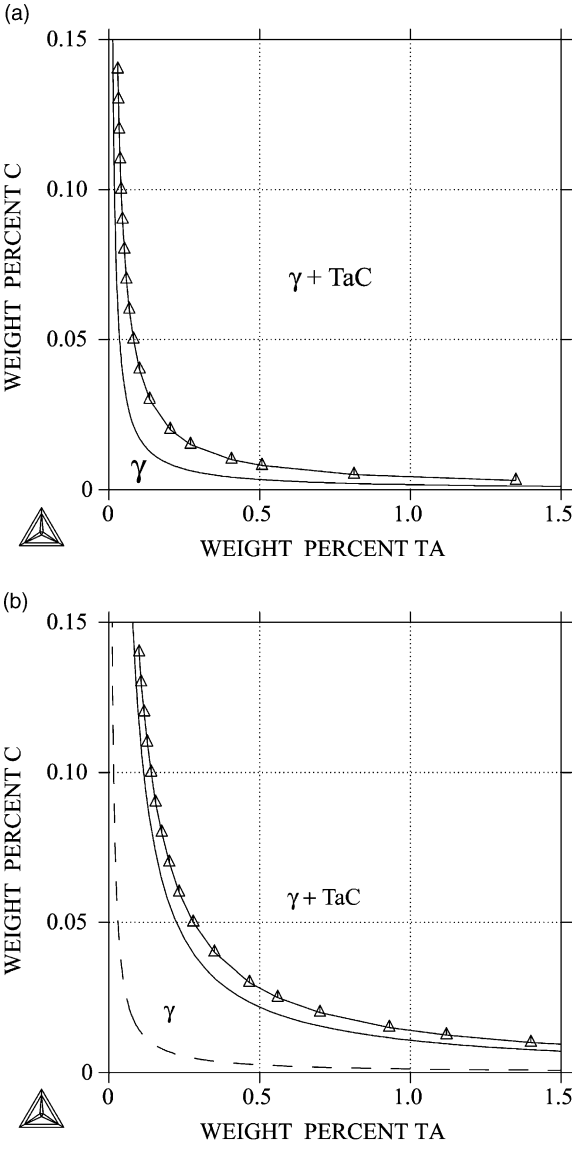

Fig. 5. Experimental data of solubility of TaC in austenite compared to Thermocalc predictions for the Fe–Ta–C system at 1050 °C (a) and 1200 °C (b). The curve in dashed line in (b) corresponds to the results of the optimization given in dashed line in Fig. 1(d). △ TaC in austenite after Narita [40].

data for the Fe–Ta system. Fig. 6 compares the curves from Tamura's et al. equation (3) to Thermocalc predictions for the composition of the Eurofer 97 alloy. Tamura's et al. alloys were similar in composition to Eurofer 97 although they made their calculations neglecting the N dissolution in TaC and assuming that TaC is a stoichiometric compound. Thus, in order to compare with their data, we have not considered the N content of the Eurofer 97 steel. It is seen that the presence of bcc-stabilizers as Ta, W or V in the steel system produces the occurrence of both a single-phase δ and a two-phase ($\delta + \gamma$) solid solution phase field in the given composition ranges. The phase diagrams for the compositions used by Tamura et al. (steels type F82H [6]) are similar to that of Fig. 6. The agreement between calculated and experimental values is less good in Fig. 6 than in Fig. 5. This is probably due to the influence of alloying elements on the solubility product of carbides in austenite. The presence of δ-ferrite (stabilized by those alloying elements) could also play a role in this behavior of carbides. The presence of δ-ferrite after heat treatment at temperatures equal or higher than 1050 °C has been experimentally determined for different 9Cr steel compositions [2,6].

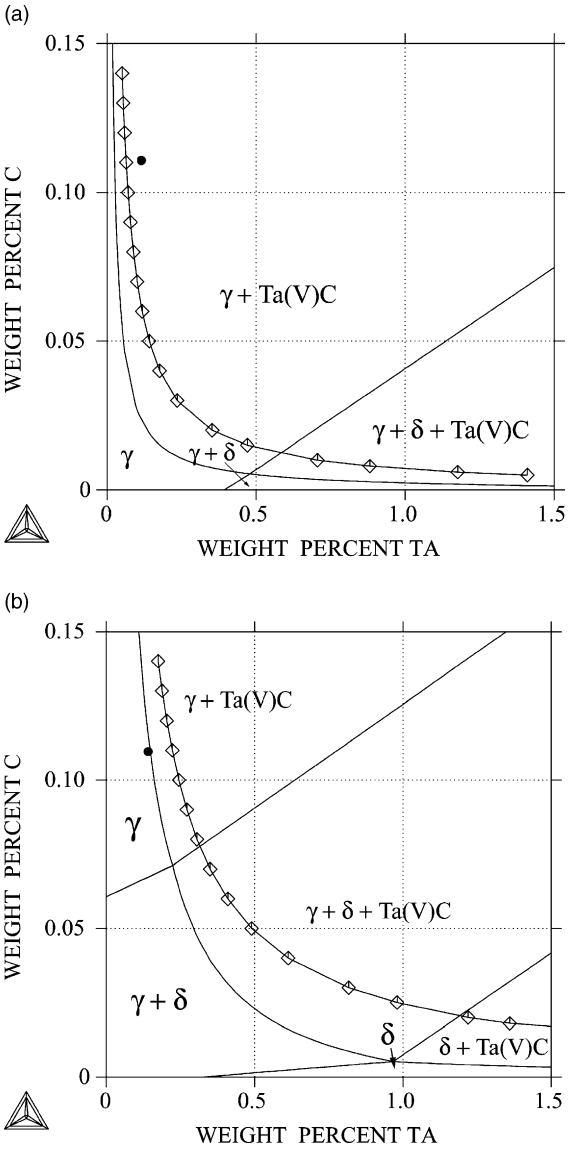

Fig. 6. Experimental data of solubility of TaC in austenite compared to Thermocalc predictions for the composition of the Eurofer 97 alloy (without N) at 1050 °C (a) and 1200 °C (b). δ stands for ferrite. The black dot shows the approximate composition of the alloy in C and Ta. ◇ TaC in austenite after Tamura [6].

The influence of alloying elements on the solubility could be taken into account by repeating the same procedure used to model the Fe–Ta binary system with other binary systems involving Fe and those elements such as Fe–V, Fe–Cr and Fe–W. At the same time, new experimental determinations on systems like Ta–V and Ta–W should contribute to a more accurate thermodynamic description of them.

The comparison of experimental data in Figs. 5 and 6 shows that, under the assumptions made in Ref. [6] to calculate the solubility product, the solubility of TaC is enhanced by the addition of alloying elements with respect to the ternary FeTaC alloy. Despite the above mentioned drawbacks, this tendency is correctly predicted by Thermocalc.

3.2.2. Calculated equilibrium solubility of Ta-rich nitrides in austenite

Fig. 7 shows the solubility curves for the TaN nitride calculated by Thermocalc compared to those obtained from the two expressions of the solubility product, given by Narita [40] and Mori [41] for ternary FeTaN alloys. It must be noted that the predicted nitride as well as the observed one is the hcp one and that Eqs. (5) and (6) above give a considerably different result on solubility at 1200 °C.

In this point it is worth to mention that the fcc δ-TaN_x nitride is not stable below 1950 K in the binary Ta–N system [14]; the equilibrium phase of TaN formed at lower temperatures is hcp ε-TaN. However, many experimental results have shown that the fcc nitride could be stabilized at low temperatures by adding small amounts of carbon [45].

3.2.3. Decomposition temperature of (Ta,V)(C,N) carbonitride in the case of the Eurofer 97 alloy

Phase equilibria were calculated in step scans 'on cooling' to investigate the possible unmixing of the (Ta,V) carbonitride fcc phase into a VN-like phase and a TaC-like phase. For this calculation to be carried out, it was necessary to introduce a third fcc structure identical

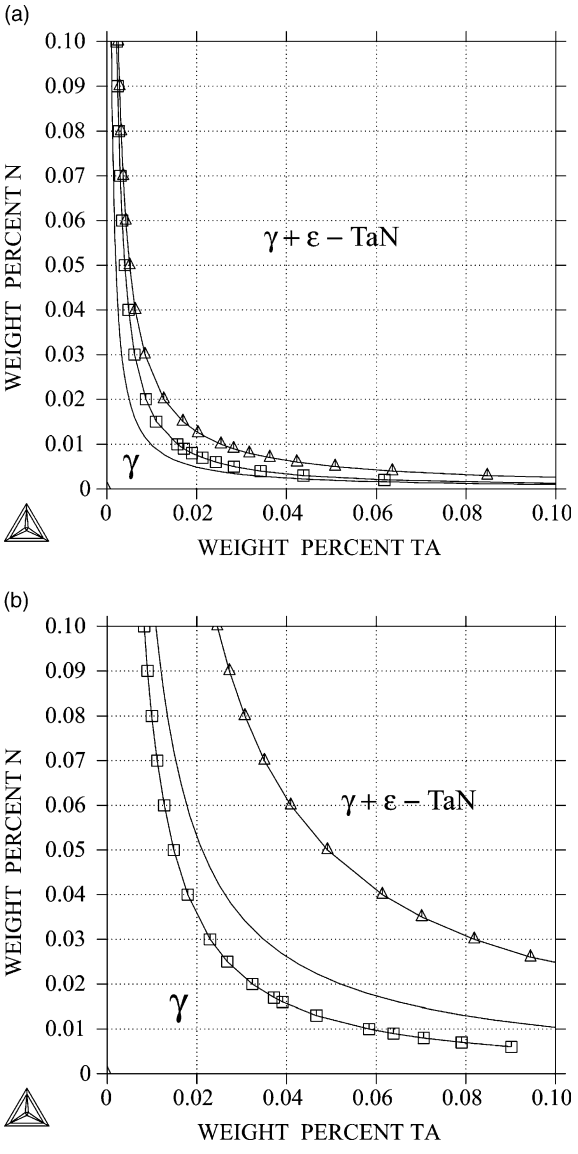

Fig. 7. Experimental data of solubility of TaN in austenite compared to Thermocalc predictions for the Fe–Ta–N system at 1050 °C (a) and 1200 °C (b). △ TaN in austenite after Narita [40], □ $TaN_{0.85}$ in austenite after Mori [41].

to that described in Section 2.1.3 above. This procedure has been already suggested in the steel literature [46]. The occurrence of such a decomposition, for which a V(Ta)N(C) and a Ta(V)C(N) phase are formed, was effectively calculated at 1018 °C working with the updated database. However, for the sake of simplicity, we will report in what follows the results of calculations performed in the austenite region at temperatures above this second unmixing temperature, that is, allowing for unmixing to occur only with two fcc structures.

3.2.4. Equilibrium solubility of Ta-rich carbonitrides in austenite of the Eurofer 97 alloy

Fig. 8 displays the equilibrium phase relationships for Eurofer 97 calculated by Thermocalc at 1050 and 1200 °C. We have evaluated the carbonitride solubility for one fixed N composition, that is, the alloy composition. It is important to point out that the fcc

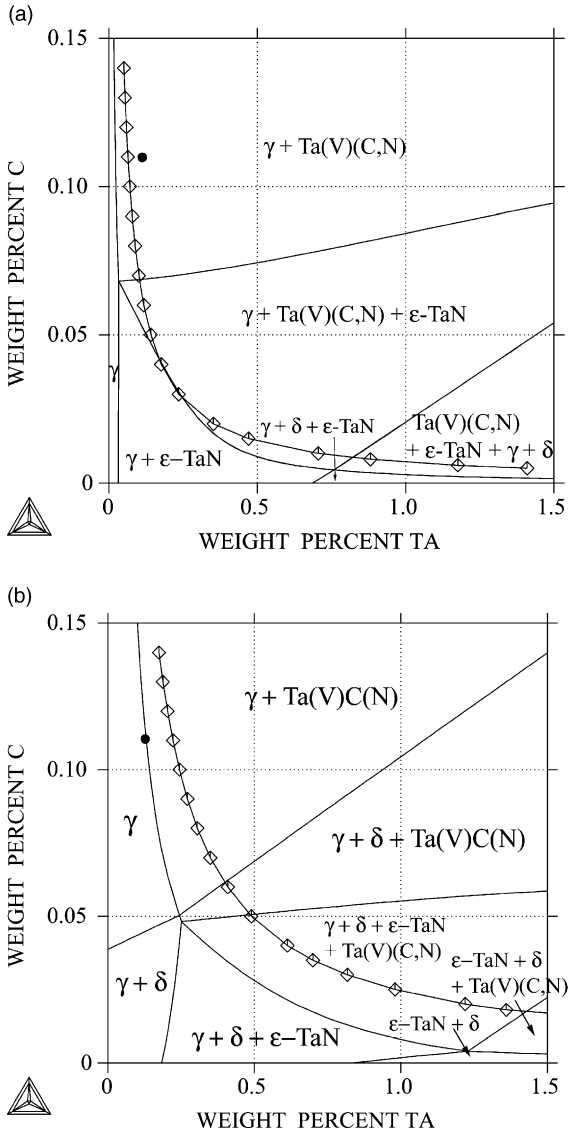

Fig. 8. Experimental data of solubility of fcc TaC in austenite compared to Thermocalc predictions for the Eurofer 97 alloy including the fcc (Ta,V)(C,N) carbonitride at $T = 1050$ °C (a) and 1200 °C (b). The N content is fixed at the original 0.022 wt% value. δ stands for ferrite. The black dot shows the approximate composition of the alloy in C and Ta. ◇ TaC in austenite after Tamura [6].

carbonitride is predicted to coexist with the hcp nitride and that, as in the precedent case, there is a composition range for which the solid solution phase field is a two-phase field. We have added the experimental curve for TaC from Tamura [6] for comparison. It is also worth to note that Thermocalc predicts at 1200 °C two different forms of the carbonitride, namely, a Ta(V)C(N) with only traces of N (for carbon contents approximately higher than 0.05) and a 'true' carbonitride Ta(V)(C,N).

Complementary calculations have shown that increasing the N content shifts the solubility curve, expanding the ($\gamma + \varepsilon$-TaN) or ($\gamma + \delta + \varepsilon$-TaN) phase field. In other words, higher N contents stabilize the ε-TaN phase with respect to the carbonitride phase.

4. Conclusions

The addition of the optimized thermodynamic parameters of the various phases formed with the major alloying elements of low activation steels to the existing database TCFe2000 enabled us to make a first contribution to establish a steel database including Ta and to calculate phase equilibria for the Eurofer 97 alloy. The homogenization of the thermodynamic descriptions of the phases in sublattices was necessary, in particular for the μ phase of the binary Fe–Ta system, in order to preserve the coherence with the μ phases of other systems included in the database. A complete reassessment of the binary Fe–Ta system was done which was also consistent with the solubility data in the ternary Fe–Ta–C and Fe–Ta–N systems. An optimization of the multicomponent systems comprising Ta would be necessary in the future, which in turn implies new experimental determinations. However, excess parameters of the order higher than 3 are expected to give a weak influence on the calculations.

The calculations carried out with Thermocalc and the updated database showed a reasonable agreement with the experimental results available in the literature in the case of the binary Fe–Ta system and the austenite region of ternary alloys. Thermocalc can provide a useful tool of prediction of phase equilibria, in particular with regard to the dissolution or precipitation of carbides, nitrides or carbonitrides in the austenite or (austenite + ferrite) phase fields.

Acknowledgements

This work has been performed under Contract CEA-CEPHYTEN No. SAV 29135/VCH between the Commissariat à l'Energie Atomique (CEA-Saclay) and the Université de Paris Sud (France).

Appendix A

New optimized thermodynamic parameters for the Fe–Ta binary system. The energies are given in J/mol, T in K.

Liquid phase

Description: (Fe,Ta)

$$^{0}L^{\text{liq.}}_{\text{Fe,Ta}} = -35\,806.85 + 6.67T,$$

$$^{1}L^{\text{liq.}}_{\text{Fe,Ta}} = -7151.11 + 8.36T,$$

$$^{2}L^{\text{liq.}}_{\text{Fe,Ta}} = -25\,785.04 + 6.19T.$$

FCC-A1 phase

Description: (Fe,Ta)(Va)

$$^{0}G^{\text{fcc}}_{\text{Ta:Va}} - {}^{0}H^{\text{bcc}}_{\text{Ta}}(298.15\text{ K}) = 16\,000 + 1.7T + \text{GHSERTa}^{+},$$

$$^{0}L^{\text{fcc}}_{\text{Fe,Ta:Va}} = -3137.0 - 9.12T.$$

$^{+}$ GHSER stands for G-HSER quoted in Ref. [22].

BCC-A2 phase

Description: $(\text{Fe,Ta})(\text{Va})_3$

$$^{0}G^{\text{bcc}}_{\text{Ta:Va}} - {}^{0}H^{\text{bcc}}_{\text{Ta}}(298.15\text{ K}) = \text{GHSERTa},$$

$$^{0}L^{\text{bcc}}_{\text{Fe,Ta:Va}} = 8770.23 + 2.46T,$$

$$^{1}L^{\text{bcc}}_{\text{Fe,Ta:Va}} = -16\,912.44 + 0.228T.$$

ε Laves phase (C14)

Description: $(\text{Fe,Ta})_2$ (Fe,Ta)

$$^{0}G^{\text{Laves}}_{\text{Fe:Fe}} - 3{}^{0}H^{\text{bcc}}_{\text{Fe}}(298.15\text{ K}) = +15\,000 + 3\text{GHSERFe},$$

$$^{0}G^{\text{Laves}}_{\text{Ta:Ta}} - 3{}^{0}H^{\text{bcc}}_{\text{Ta}}(298.15\text{ K}) = +15\,000 + 3\text{GHSERTa},$$

$$^{0}G^{\text{Laves}}_{\text{Ta:Fe}} - 2{}^{0}H^{\text{bcc}}_{\text{Ta}}(298.15\text{ K}) - {}^{0}H^{\text{bcc}}_{\text{Fe}}(298.15K) = 30\,000 + 105\,310.45 - 35.2T + \text{GHSERFe} + 2\text{GHSERTa},$$

$$^{0}G^{\text{Laves}}_{\text{Fe:Ta}} - 2{}^{0}H^{\text{bcc}}_{\text{Fe}}(298.15\text{ K}) - {}^{0}H^{\text{bcc}}_{\text{Ta}}(298.15\text{ K}) = -105\,310.45 + 35.2T + 2\text{GHSERFe} + \text{GHSERTa},$$

$$^{0}L^{\text{Laves}}_{\text{Fe,Ta:}*} = 45\,970 - 6.6T,$$

$$^{0}L^{\text{Laves}}_{*\text{:Fe,Ta}} = -14\,914 + 14.6T. \quad (7)$$

μ phase

Description: $(Fe,Ta)_7\ Ta_2(Fe,Ta)_4$

$$
\begin{aligned}
&{}^0G^{\mu}_{Fe:Ta:Fe} - 11\,{}^0H^{bcc}_{Fe}(298.15\ K) - 2\,{}^0H^{bcc}_{Ta}(298.15\ K)\\
&\quad = -65\,000 + 3\,173\,211.95 - 115.56T - 393\,068.11\\
&\qquad + 117.39T + 7GFCCFe + 4GHSERFe\\
&\qquad + 2\ GHSERTa,
\end{aligned}
$$

$$
\begin{aligned}
&{}^0G^{\mu}_{Ta:Ta:Fe} - 4\,{}^0H^{bcc}_{Fe}(298.15\ K) - 9\,{}^0H^{bcc}_{Ta}(298.15\ K)\\
&\quad = 3\,173\,211.95 - 115.56T + 4GHSERFe\\
&\qquad + 9GHSERTa,
\end{aligned}
$$

$$
\begin{aligned}
&{}^0G^{\mu}_{Fe:Ta:Ta} - 7\,{}^0H^{bcc}_{Fe}(298.15\ K) - 6\,{}^0H^{bcc}_{Ta}(298.15\ K)\\
&\quad = -393\,068.11 + 117.39T + 7GFCCFe\\
&\qquad + 6GHSERTa,
\end{aligned}
$$

$$
{}^0L^{\mu}_{Fe,Ta:Ta:*} = 43\,319.562 + 55.5326T,
$$

$$
{}^0L^{\mu}_{*:Ta:Fe,Ta} = 238\,945.5705 + 110.0088T.
$$

* Stands either for Fe or Ta.

References

[1] R.L. Klueh, J. Met. 44 (1992) 20.
[2] F. Abe, T. Noda, M. Okada, J. Nucl. Mater. 195 (1992) 51.
[3] R. Jarayam, R.L. Klueh, Metall. Mater. Trans. 29A (1998) 1551.
[4] Y. de Carlan, A. Alamo, M.H. Mathon, G. Geoffroy, A. Castaing, J. Nucl. Mater. 283–287 (2000) 672.
[5] A. Alamo, J.C. Brachet, A. Castaing, C. Lepoittevin, F. Barcelo, J. Nucl. Mater. 258–263 (1998) 1228.
[6] M. Tamura, K. Shinozuka, K. Masamura, K. Ishizawa, S. Sugimoto, J. Nucl. Mater. 258–263 (1998) 1158.
[7] P. Fernández, A.M. Lancha, J. Lapeña, M. Hernández-Mayoral, Fusion Eng. Design 58–59 (2001) 787.
[8] A. Danon, A. Alamo, J. Nucl. Mater. 307–311 (2003) 479.
[9] R. Lindau, M. Schirra, Fusion Eng. Design 58–59 (2001) 781.
[10] A. Danon, C. Servant, A. Alamo, J.C. Brachet, Mater. Sci. Eng. 348 (2003) 122.
[11] L. Kaufman, H. Bernstein, Computer Calculations of Phase Diagrams, Academic Press, New York, NY, 1970.
[12] B. Sundman, J. Ågren, J. Phys. Chem. Solids 42 (1981) 297.
[13] K. Frisk, A. Fernández Guillermet, J. Alloys Comp. 238 (1996) 167.
[14] K. Frisk, J. Alloys Comp. 278 (1998) 216.
[15] N. Dupin, I. Ansara, J. Phase Eq. 14 (1993) 451.
[16] N. Dupin, I. Ansara, Z. Metallkd. 87 (1996) 555.
[17] L. Kaufman, P.E.A. Turchi, W. Huang, Z.K. Liu, Calphad 25 (2001) 419.
[18] C. Vahlas, P.Y. Chevalier, E. Blanquet, Calphad 13 (1989) 273.
[19] L. Kaufman, Calphad 15 (1991) 243.
[20] S. Srikanth, A. Petric, J. Alloys Comp. 203 (1994) 281.
[21] G.C. Coelho, S.G. Fries, H.L. Lukas, P. Majewski, J.M. Zelaya Bejarano, S. Gama, C.A. Ribeiro, G. Effenberg, in: P. Kumar, H.A. Jehn, M. Uz (Eds.), Processing and Applications of High Purity Refractory Metals and Alloys, The Minerals, Metals and Materials Society, Warrendale, USA, 1994, p. 51.
[22] A.T. Dinsdale, Calphad 15 (1991) 317.
[23] O. Redlich, A. Kister, Industr. Eng. Chem. 40 (1948) 345.
[24] C. Wagner, W. Schottky, Z. Phys. Chem. 11 (1930) 163.
[25] N. Saunders, private communication, 1992.
[26] J.G. Costa Neto, S.G. Fries, H.L. Lukas, S. Gama, G. Effenberg, Calphad 17 (1993) 219.
[27] S. Akamatsu, M. Hasebe, T. Senuma, Y. Matsumura, O. Akisue, ISIJ Int. 34 (1994) 9.
[28] W. Stuckens, A. Michel, Bull. Chim. Soc. Fr. (1962) 1541.
[29] W. Stuckens, Ann. Chim. (Paris) 8 (1963) 229.
[30] B.J. Lee, Metall. Mater. Trans. 32A (2001) 2423.
[31] M. Iguchi, S. Nosomi, K. Saito, T. Fuwa, J. Iron Steel Inst. Jpn. 68 (1982) 633.
[32] V.S. Sudavtsova, V.P. Kurach, G.I. Batalin, Izv. Akad. Nauk SSSR Met. 3 (1987) 60.
[33] E. Ichise, K. Horikawa, ISIJ Int. 29 (1989) 843.
[34] A. Raman, Trans. Indian Inst. Met. 19 (1966) 202.
[35] G.C. Coelho, J.G. Costa Neto, S. Gama, C.A. Ribeiro, J. Phase Eq. 16 (1995) 121.
[36] W.A. Fischer, K. Lorez, H. Fabritius, D. Schlegel, Arch. Eisenhüttenwes. 41 (1970) 489.
[37] E.P. Abrahamson, S.L. Lopata, Trans. Met. Soc. AIME 236 (1966) 76.
[38] A.K. Sinha, W. Hume-Rothery, J. Iron Steel Inst. 205 (1967) 671.
[39] R. Genders, R. Harrison, J. Iron Steel Inst. 134 (1936) 173.
[40] K. Narita, Trans. Iron Steel Inst. Jpn. 15 (1975) 147.
[41] T. Mori, M. Tokizane, E. Sunami, Y. Nakajima, Trans. Iron Steel Inst. Jpn. 10 (1970) 350.
[42] L.J. Swartzendruber, E. Paul, in: T.B. Massalski (Ed.), Binary Alloy Phase Diagrams, 2nd Ed., ASM International, Materials Park, Ohio, 1990, p. 1776.
[43] R.P. Elliot, W. Rostoker, Metall. Trans. ASM 50 (1958) 617.
[44] R. Wetzig, Phys. Status Solidi 27 (1968) K7.
[45] H. Wiesenberger, W. Lengauer, P. Ettmayer, Acta Mater. 46 (1998) 651.
[46] B.C. Schaffernak, H.H. Cerjak, Calphad 25 (2001) 241.